JOURNAL OF CATALYSIS 128, 186–197 (1991)

Reversal of the SMSI State on Pt/TiO_2 by CO Hydrogenation

KATHERINE J. BLANKENBURG AND ABHAYA K. DATYE[1]

Department of Chemical and Nuclear Engineering, University of New Mexico, Albuquerque, New Mexico 87131

Received September 19, 1989; revised October 4, 1990

We have examined the role of the SMSI state in the CO hydrogenation activity of Pt/TiO_2 and, in particular, whether CO hydrogenation leads to reversal of the SMSI state. Hydrogenolysis of *n*-butane, which is suppressed in the SMSI state, was used to monitor the onset and reversal of the SMSI state. When CO hydrogenation was performed on a Pt/TiO_2 catalyst subjected to high temperature reduction, there was almost a complete restoration of hydrogenolysis activity. This implies that the working catalyst surface during CO hydrogenation is free of the site-blocking oxide species responsible for the SMSI state. The ratio of hydrogenolysis/isomerization activity of *n*-butane was also unaffected by onset of the SMSI state. Therefore, the migration of TiO_x over the metal surface during SMSI does not cause selective suppression of hydrogenolysis with respect to isomerization. The site-blocking oxide species responsible for SMSI on the metal surface do not appear to be necessary to obtain enhanced CO hydrogenation activity on Pt/TiO_2.

INTRODUCTION

Since the SMSI phenomenon was first reported by Tauster *et al.* (*1*), a great deal of evidence has accumulated in the literature showing that the chemisorptive and catalytic properties of titania-supported metals are affected by high temperature reduction (HTR). For instance, HTR leads to a loss of H_2 and CO chemisorption ability and a pronounced drop in hydrogenolysis reactivity after HTR (*2–5*). On the other hand, titania-supported metals are more reactive for the CO hydrogenation reaction (*6–10*). The drop in hydrogenolysis activity and chemisorption ability is explained by migration of TiO_x onto the metal to cause site blocking (*11, 12*), but that is difficult to reconcile with the increase in CO hydrogenation activity on the same surface. It has been suggested that special sites at the metal–oxide interface are responsible for this enhanced reactivity (*8*). Since high temperature reduction causes migration of Ti-suboxide species onto the metal surface (*11, 12*), it should also lead to an increase in the number of these special interfacial sites. Hence, one would expect an inverse correlation between hydrogenolysis activity and CO hydrogenation rate. In our previous work on TiO_2-supported Rh (*5*), we failed to detect such a correlation. To examine this aspect in greater detail, and to investigate the connection between the SMSI state and enhanced CO hydrogenation activity, we have studied the behavior of TiO_2-supported Pt exposed to HTR.

The reports in the literature on whether HTR (and the SMSI state) is necessary to obtain the enhanced reactivity in CO hydrogenation on titania supports are conflicting. When TiO_2 was deposited on Pt metal powder (*13*) or on single crystals of Rh (*14*), there was a definite enhancement of CO hydrogenation reactivity even without any high temperature reduction. The work on supported catalysts shows either no effect (*5, 8*) or a major effect of HTR (*9, 10*) on reactivity. A major complication in the determination of turnover frequencies (TOF)

[1] To whom correspondence should be addressed.

0021-9517/91 $3.00

on supported catalysts in the HTR state is the marked drop in H_2 uptake after HTR. If this suppressed uptake of H_2 is used as a measure of the number of surface sites on the catalyst, one can get erroneously high TOFs. The question of whether the catalyst remains in the SMSI state during CO hydrogenation is largely unanswered. Data presented by Wang *et al.* (*9*) imply that the catalyst is still in the SMSI state after reaction since both H_2 uptake and the coverage of CO measured by IR remained low. On the other hand, Anderson and Burch (*15*) reported a 22% reversal of the SMSI state (as determined by H_2 chemisorption) after exposing the Pt/TiO_2 catalyst to CO/H_2 reaction conditions for 30 min.

There is some concern about the accuracy of H_2 chemisorption measurements for measuring exposed metal atoms in the SMSI state since spillover of the H_2 to the support can occur. Other surface analytical techniques such as AES and ISS are difficult to apply to a working catalyst to infer the onset of SMSI. Therefore, in this study, we have used *n*-butane hydrogenolysis as a reactive probe to monitor the onset and reversal of the SMSI state. In previous work on Rh/TiO_2, we observed that *n*-butane hydrogenolysis was very sensitive to onset of the SMSI state: there was a 3 orders of magnitude drop in reactivity after HTR (*5*). Oxidation of the catalyst at 573 K led to complete restoration of activity. The reversibility of the activity changes suggested that they were related to site blocking due to a migration of Ti-suboxide species over the metal after HTR and their removal by oxidation. This was confirmed by high resolution TEM in the profile imaging mode (*16*). However, hydrogenolysis activity is known to be affected by particle size and also by the morphological changes induced by oxidation–reduction cycles (*17, 18*). In this study, by comparing the results on TiO_2-supported Pt with those on other supports, we hope to separate the effect of particle size and morphology and identify factors that are unique to the TiO_2 support. Furthermore, on Pt, the isomerization of *n*-butane occurs along with hydrogenolysis. Isomerization reactions are generally considered to be structure insensitive and literature reports show that *n*-butane isomerization activity is not affected by particle size (*19*) and only modestly affected by surface structure (*20*). Hence, the isomerization activity provides us with a probe that is insensitive to particle size and morphology and should be affected by TiO_x surface coverage alone.

We report here the influence of oxidation–reduction cycles on the reactivity of Pt supported on SiO_2, TiO_2, and Al_2O_3. By performing CO hydrogenation and *n*-butane hydrogenolysis in succession on the same catalyst, we have been able to monitor the state of the working catalyst surface during CO hydrogenation (post-SMSI). The evidence suggests that CO hydrogenation leads to removal of TiO_x species from the metal surface and restoration of hydrogenolysis and isomerization activity. The site-blocking TiO_x species do not appear to be necessary for the enhanced CO hydrogenation activity since they are quite efficiently cleared off the metal surface by the CO hydrogenation reaction.

EXPERIMENTAL

Three supports were used in this study. The TiO_2 used was Degussa P25 titanium dioxide with a purity of 99.5% TiO_2, primarily in the anatase form, having a BET surface area of 50 m^2/g and an average particle diameter of 30 nm. The SiO_2 used was Aesar silica gel catalyst support with a purity of 99.5% and a BET surface area of 425 m^2/g. The Al_2O_3 used was Degussa aluminum oxide C, which has a purity of 99.6%, a BET surface area of 100 m^2/g, and an average particle diameter of 20 nm.

The CO and the *n*-butane were Matheson research purity, 99.99 and 99.9%, respectively. The CO was further purified to remove carbonyl compounds by running it through a trap containing glass beads heated to 600 K, followed by ascarite and a 7-μm Swagelok particle filter. The other gases

used were Alphagaz UHP grade, 99.999% for He and H_2 and 99.993% for O_2.

Three different precursors were used in catalyst preparation. The chloride precursor was $H_2PtCl_6 \cdot xH_2O$ of 99.995% purity. The "acac" precursor was platinum(II) acetylacetonate (2,4-pentanedionate, platinum(II) derivative) of 97% purity. The amine precursor was $Pt(NH_3)_4Cl_2$ of 99.99% purity. All three were supplied by Aldrich Chemical Co. The solvent used for nonaqueous impregnation was acetonitrile (Fisher HPLC grade, 99.9%). All impregnation used 1 ml of solvent per gram of support. The catalysts were dried overnight in air at 393 K. The acac- and chloride-derived catalysts were calcined prior to reduction using 10% O_2 in He at 22.3 SCCM for 1 hr at 323 K, followed by a 1.5-hr temperature ramp to 493 K, held for 4 hr and cooled to room temperature. After purging with flowing He at 20 SCCM for 15 min, the catalyst was then reduced in flowing H_2 by increasing the temperature to 393 K over 1 hr, holding for 1 hr, ramping to 493 K over 2 hr, holding for 4 hr, ramping to 673 K for 2 hr, and holding for 4 hr.

The catalysts used in this study came from a larger study aimed at understanding the role of pretreatment and catalyst preparation conditions in the reactivity of Pt (*21*). It was assumed that the catalysts prepared using the acac precursor with nonaqueous impregnation would lead to minimal dissolution of the alumina and titania supports, while the chloride precursor with water as solvent might lead to etching of the support. Observations of the chloride-impregnated catalyst by TEM confirmed that oxide dissolution had occurred during the catalyst preparation, leading to possible deposition of oxide species on the metal surface (*22*). However, when the chloride-derived catalyst was calcined prior to reduction, the metal surface appeared to be devoid of amorphous overlayers. Calcination seems to minimize the contamination of the metal surface by support-derived oxide species and hence the calcined catalyst (PtT12a) was used in this study. Aqueous impregnation of the silica with the chloride precursor led to precipitation of Pt and a poorly dispersed catalyst. Hence, catalyst PtSO4 was prepared by an ion exchange technique (*23*) using the amine precursor on silica gel and maintaining the pH at 8.5. The results on both the acac- (PtT04) and the chloride-derived (PtT12a) Pt/TiO_2 catalysts are compared with the silica-(PtSO4) and alumina-supported catalysts (PtAl01) to investigate the role of HTR in CO hydrogenation activity. The characterization results on these catalysts are summarized in Tables 1 and 2.

The number of active Pt sites per gram on the fresh catalyst were determined by the static volumetric chemisorption uptake of H_2. The samples were reduced overnight at 673 K in 200 Torr of static H_2. Pressure was monitored by an MKS Baratron pressure head with a type 170 M-6C range multiplier connected to a Keithley 179 TRMS digital multimeter. An adsorption stoichiometry of $H/Pt_s = 1$ was assumed. Reactivity measurements were performed in a quartz U-tube differential flow reactor. Prereduced catalysts were reduced at 673 K in flowing H_2 for 30 min prior to reaction. Reaction products were analyzed by a Hewlett–Packard Model HP 5890 gas chromatograph with a 10-ft Haysep Q column, a thermal conductivity detector, and a Model HP 3392a integrator. Differences in detector sensitivity for the products were accounted for by the use of relative response factors, either calculated from a calibration gas mixture (Scott Gases) or from literature values (*24*). Conversions were kept below 10% to ensure differential operation of the reactor.

Hydrogenolysis of *n*-butane was carried out at a flow rate of 21 SCCM with a feed ratio of 20 H_2/1 *n*-butane and a pressure of 84.8 kPa. Reactants were allowed to flow for 10 min to achieve steady state conditions before being sampled. After analysis, the catalyst was reduced in flowing H_2 at 20 SCCM for 10 min at the reaction tempera-

TABLE 1

Summary of Catalysts Used

Code	Wt% Pt	Precursor	Support	Solvent	Pretreatment
PtTO4	2	$Pt(acac)_2$	TiO_2	CH_3CN	Calcination
PtT12a	4	$H_2PtCl_6 \cdot xH_2O$	TiO_2	H_2O	Calcination
PtAlO1	2	$Pt(acac)_2$	Al_2O_3	CH_3CN	Calcination
PtSO4	4	$Pt(NH_3)_4Cl_2$	SiO_2	H_2O	None

ture in order to remove any carbon deposits from the surface before proceeding to the next reaction. CO hydrogenation was carried out at a flow rate of 20 SCCM and a feed ratio of $H_2/CO = 3.0$ at a total pressure of 84.8 kPa. Again, reaction was carried out for 10 min to achieve steady state and followed by a minimum of 10 min reduction with H_2 at 15 SCCM at reaction temperature before the next reaction.

Reactivity measurements were done at various temperatures on the fresh catalyst. An Arrhenius plot was determined for each catalyst, first for *n*-butane hydrogenolysis, then for CO hydrogenation, in order to calculate activation energies. Typically, several runs were done at each temperature to ensure reproducibility of results. These activation energies were then used to normalize all turnover frequencies to a reference temperature of 553 K. After studying the reactivity of the catalyst in the fresh state, the reactivities in the oxidized state and in the HTR state were measured. In all instances, reactivity measurement consisted of performing *n*-butane hydrogenolysis before and after CO hydrogenation. Each catalyst went through the following sequence of treatments: fresh H_2-reduced (673 K), oxidized, HTR, oxidized, HTR, and so on for several cycles. The oxidation treatment was performed with 10% O_2 in helium at a flow rate of 22.3 SCCM at 823 K for 2 hr. After purging in helium for 15 min, the catalyst was reduced for 30 min at reaction temperature before reactivity measurements were begun. The high temperature reduction treatment was performed by treat-

TABLE 2

Characterization of the Catalysts Used

	Hydrogen chemisorption (μmol/g catalyst)		Particle diameter (nm) measured by TEM		TOF$*10^4$ (sec^{-1}) for hydrogenolysis[a]		TOF$*10^4$ (sec^{-1}) for isomerization		TOF$*10^4$(sec^{-1}) for CO hydrogenation	
	Before[b]	After[c]	Before	After	Before	After	Before	After	Before	After
PtSO4	102	18.8	1.3	4.0	9.1	3.8	0.58	4.7	3.9	18.5
PtAlO1	27.5	6.2	1.0	15.6	7.6	2.4	0.98	1.6	20.0	29.3
PtTO4	18.1	9.8	1.5	2.2	3.4	7.1	0.82	2.4	136.4	233.3
PtT12a	43.3	20.9	1.3	2.0	4.1	9.4	0.40	1.2	123.2	178.9

[a] All TOFs are expressed at a reference temperature of 553 K and a pressure of 84.8 kPa with a feed ratio of H_2/*n*-butane = 20 and $H_2/CO = 3$.

[b] "Before" refers to the catalyst in its initial state, i.e., after H_2 reduction at 673 K.

[c] "After" refers to the catalyst after removal from the reactor upon completion of the oxidation–reduction cycles and activity measurements. TOFs are reported for the last oxidized state before the catalyst was removed.

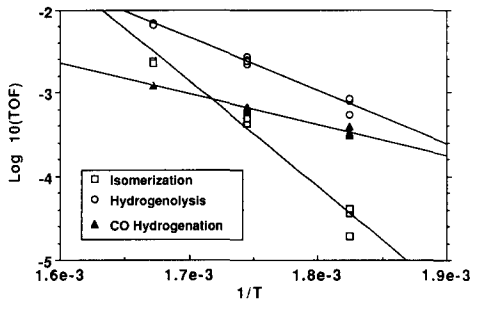

FIG. 1. Arrhenius plot for (▲) CO hydrogenation (H_2/CO = 3, P = 84.8 kPa) and (○) n-butane hydrogenolysis and (□) isomerization (H_2/butane = 20, P = 84.8 kPa).

ing the catalyst in flowing H_2 at 773 K for 2 hr.

RESULTS

Pt/SiO_2

Figure 1 shows the Arrhenius plot for n-butane hydrogenolysis and for CO hydrogenation on the fresh catalyst PtSO4. The activation energies are 243 kJ/mol for isomerization, 124 kJ/mol for hydrogenolysis, and 69.4 kJ/mol for CO hydrogenation. The turnover frequency for CO hydrogenation at 553 K, $3.9 \times 10^{-4}\ s^{-1}$, and the activation energy are in good agreement with the values reported by Vannice and Twu (*7*). At these reaction temperatures, methane is the dominant hydrocarbon product. The activation energy and TOF for n-butane hydrogenolysis are also in good agreement with those reported by Rodríguez-Reinosos *et al.* (*19*). The differences in activation energy for isomerization and hydrogenolysis lead to increased selectivity for isomerization at higher temperatures.

Figure 2 shows the reactivity of PtSO4 at 553 K for n-butane hydrogenolysis, isomerization, and CO hydrogenation as a function of treatment. To ensure reproducibility, several runs were done at each state and the estimated error is no more than ±0.1 units on the ordinate. Every point in Fig. 2 represents the average of several runs after extrapolation to 553 K. Since chemisorption uptake could not be measured *in situ*, the turnover frequency could not be reported after every pretreatment. Therefore the activity is reported in Fig. 2 as μmol/g catalyst/sec. However, the chemisorption uptake was measured on the fresh and used catalyst and is reported in Table 2 and can be used to derive a TOF for the fresh and cycled catalysts. The experimental error in the TOF values arises mainly from the uncertainties in chemisorption uptake from the small aliquot of catalyst recovered from the reactor after reactivity measurements. Hence, variations in TOF values reported in Table 2 within a factor of 2 should be considered insignificant and within the limits of experimental error.

The data show that n-butane hydrogenolysis activity per gram declines significantly as the catalyst is progressively cycled. The drop in hydrogenolysis is caused by sintering and loss of metal surface area. The fresh catalyst had a mean Pt particle diameter of 1.3 nm. When the catalyst was removed from the reactor and examined in the TEM, the mean particle diameter was found to be 4.0 nm (*21*). The TOF for n-butane hydrogenolysis at 553 K dropped from 9.1×10^{-4} to $3.8 \times 10^{-4}\ s^{-1}$ after cycling. The isomerization activity actually increased

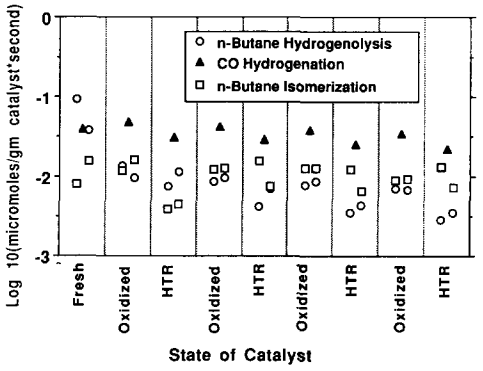

FIG. 2. Reaction rate as a function of catalyst pretreatment for PtSO4 at T_{ref} = 553 K and P = 84.8 kPa (○, n-butane hydrogenolysis before and after CO hydrogenation; □, n-butane isomerization before and after CO hydrogenation; ▲, CO hydrogenation).

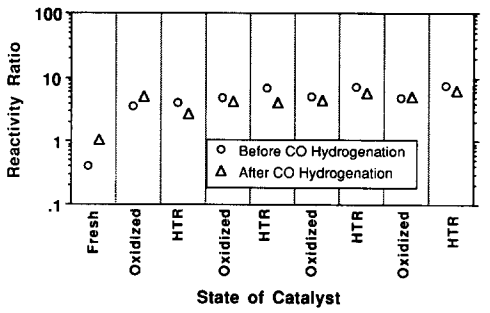

FIG. 3. Plot of the reactivity ratio (CO hydrogenation/*n*-butane hydrogenolysis) for PtSO4 at T_{ref} = 553 K and P = 84.8 kPa using *n*-butane hydrogenolysis reactivities before and after CO hydrogenation (○, *n*-butane hydrogenolysis before CO hydrogenation; △, *n*-butane hydrogenolysis after CO hydrogenation).

after sintering and the TOF at 553 K changed from 0.6×10^{-4} to 4.7×10^{-4} s^{-1}. The increase in isomerization selectivity with particle growth is consistent with the literature data on *n*-butane hydrogenolysis (*19*).

While the *n*-butane hydrogenolysis activity per gram catalyst decreased due to the oxidation–reduction cycling, the CO hydrogenation activity per gram did not change significantly. As a result, when the drop in metal surface area is taken into account, the CO hydrogenation TOF at 553 K increased from 3.9×10^{-4} s^{-1} on the fresh catalyst to 18.5×10^{-4} s^{-1} on the cycled catalyst. These data therefore show a modest increase in TOF with increasing particle diameter. This trend is consistent with the observation that small particles are generally less reactive than larger ones in the CO hydrogenation reaction (*25*). By plotting the ratio of CO hydrogenation activity to *n*-butane hydrogenolysis and isomerization activity, we can eliminate the influence of metal surface area changes and see more clearly the influence of pretreatment on the intrinsic reactivity ratio. We have used the activities in *n*-butane hydrogenolysis both before and after performing CO hydrogenation when computing the ratios plotted in Fig. 3. As seen from Fig. 3, catalyst pretreatment appears to have very little influence on the ratio of CO hydrogenation to *n*-butane hydrogenolysis activity. The increasing particle size, however, causes the relative efficiency of Pt for CO hydrogenation compared to *n*-butane hydrogenolysis to increase monotonically. Thus, while the fresh catalyst is approximately 0.4 times as reactive for CO hydrogenation as it is for *n*-butane hydrogenolysis, the catalyst, after being cycled under oxidizing and reducing conditions, is 8 times as reactive.

Pt/Al_2O_3

Figure 4 shows the reactivity of the 2% Pt/Al_2O_3 catalyst as a function of treatment. Oxidation–reduction cycling caused an overall decrease in activity per gram for all three reactions, indicating a pronounced loss of metal surface due to sintering. The average particle diameter as measured by TEM increased from 1.0 to 15.6 nm. The drop in chemisorption is not as dramatic and reflects the nonuniformity of this catalyst, which makes it difficult to derive an average diameter by TEM. It is possible that the fresh catalyst contained a number of large Pt particles that were undercounted in the TEM micrographs. The TOF for *n*-butane

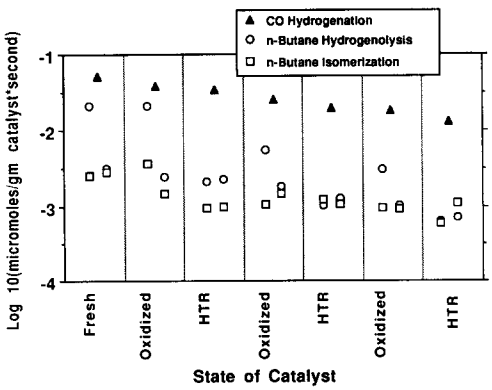

FIG. 4. Reaction rate as a function of catalyst pretreatment for PtAlO1 at T_{ref} = 553 K and P = 84.8 kPa (○, *n*-butane hydrogenolysis before and after CO hydrogenation; □, *n*-butane isomerization before and after CO hydrogenation; ▲, CO hydrogenation).

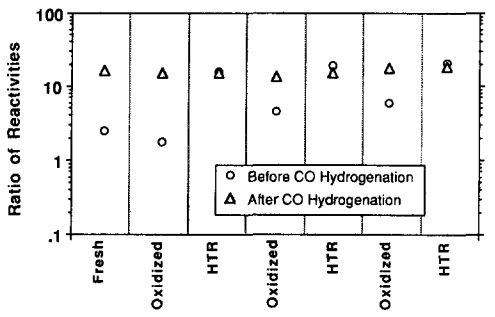

FIG. 5. Plot of the reactivity ratio for PtAlO1 at T_{ref} = 553 K and P = 84.8 kPa using n-butane hydrogenolysis reactivities before and after CO hydrogenation (□, μmol CO/μmol hydrogenolysis before CO hydrogenation; △ μmol CO/μmol hydrogenolysis after CO hydrogenation).

hydrogenolysis dropped from 7.6×10^{-4} to 2.4×10^{-4} s^{-1} over three oxidation–reduction cycles, a drop that is consistent with the particle size effect in this reaction (*19*). In contrast, the isomerization TOF went from 0.9×10^{-4} to 1.6×10^{-4} s^{-1} and the CO hydrogenation TOF went from 2.0×10^{-3} to 2.9×10^{-3} s^{-1}, indicating invariance with particle diameter, within experimental error. Figure 4 shows that HTR does not cause any suppression in the activity of any of the reactions while oxidation leads to enhanced hydrogenolysis activity. In contrast to Pt/SiO_2, CO hydrogenation proceeds faster than hydrogenolysis even on the smallest particles (the fresh catalyst). This behavior is seen more clearly when we plot the ratio of CO hydrogenation activity to butane hydrogenolysis activity in Fig. 5. The fresh Pt/Al_2O_3 has a reactivity ratio ≈2.5 which increases to ≈12 after cycling. The increase is caused by particle growth, which leads to a falloff in hydrogenolysis TOF. The ratio of CO hydrogenation activity to isomerization activity is unaffected by increased particle diameter or by any surface structure changes caused by the oxidation–reduction cycling, as seen in Fig. 6. As seen in this figure, CO hydrogenation proceeds about 20 times faster than n-butane isomerization on Pt/Al_2O_3 but only 3.5 times faster on Pt/SiO_2.

Pt/TiO_2

The results on two titania-supported catalysts are discussed here. One of these catalysts, PtTO4, was prepared with the acac precursor using nonaqueous impregnation. The other one, PtT12a, was prepared with the chloride precursor using aqueous impregnation and was calcined prior to reduction. Figure 7 shows the reactivity data on catalyst PtTO4 as a function of treatment. The CO hydrogenation activity per gram was unaffected by HTR or oxidation. The n-butane hydrogenolysis activity per gram dropped approximately 2 orders of magnitude after HTR. A similar drop was also seen in the isomerization activity on this catalyst. Oxidation at 823 K restored the n-butane hydrogenolysis and isomerization activity completely. The average particle diameter on catalyst PtTO4 increased from 1.5 to 2.2 nm after two oxidation–reduction cycles. The behavior of the titania-supported catalysts is in marked contrast to that of the silica-supported catalysts, where the fresh catalyst was less active for CO hydrogenation than for butane hydrogenolysis. Catalyst PtTO4, despite having metal particles ≈1.5 nm in diameter, is ≈50 times more reactive for CO hydrogenation than for n-butane hydrogenolysis. This reactivity ratio increases to ≈1500 when the catalyst is reduced at high temperatures in H_2 due to the suppression in hydrogenolysis activity. However, when the hydrogenolysis activity is measured after the CO hydrogenation, we find it to be comparable to the activity in the oxidized state or on the fresh catalyst (Fig. 7).

The results obtained on the aqueously impregnated and calcined catalyst (PtT12a; Fig. 8) were similar to those reported above for catalyst PtTO4. The chemisorption uptake on both these catalysts before and after reaction is reported in Table 1 and can be used to derive TOFs. The TOF for n-butane

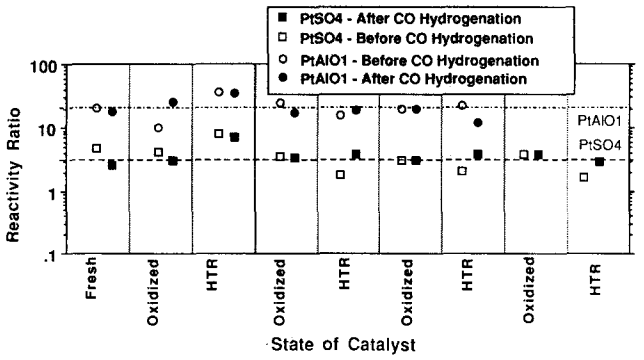

FIG. 6. Ratio of reactivities for CO hydrogenation to *n*-butane isomerization for catalysts PtSO4 and PtAlO1 at T_{ref} = 553 K and P = 84.8 kPa (□, PtSO4 before CO hydrogenation; ■, PtSO4 after CO hydrogenation; ○, PtAlO1 before CO hydrogenation; ●, PtAlO1 after CO hydrogenation).

hydrogenolysis on PtT12a at 553 K increased from 4.1×10^{-4} to 9.4×10^{-4} s^{-1}. The increase was less pronounced on catalyst PtTO4. The ratio of CO hydrogenation to butane isomerization from catalyst PtT12a is shown in Fig. 9. The ratio plot shows that this catalyst is ≈300 times more reactive for CO hydrogenation than for butane isomerization even in the fresh state (particle diameter ≈1.3 nm). However, since the butane isomerization TOF is not affected by the support (Table 2), this change must be due to an increase in the intrinsic-efficiency for CO hydrogenation on the titania-supported Pt. The further increase in this ratio after HTR is due mainly to the loss of isomerization activity in the SMSI state and not to any increase in CO hydrogenation activity. In addition, CO hydrogenation appears to undo the effects of high temperature reduction.

DISCUSSION

This study has used the hydrogenolysis and isomerization of *n*-butane as reactive probes to monitor the surface of Pt during oxidation–reduction cycles. Hydrogenolysis is generally accepted to be a structure-

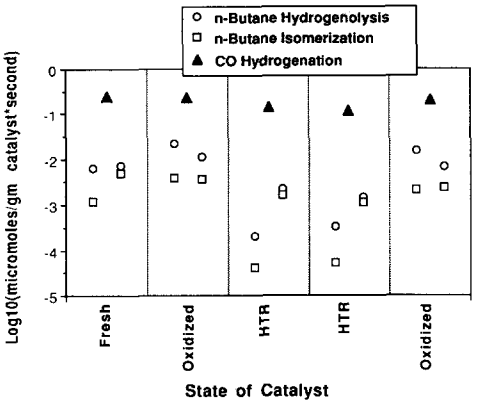

FIG. 7. Reaction rate as a function of catalyst pretreatment for PtTO4 at T_{ref} = 553 K and P = 84.8 kPa (○, *n*-butane hydrogenolysis before and after CO hydrogenation; □, *n*-butane isomerization before and after CO hydrogenation; ▲, CO hydrogenation).

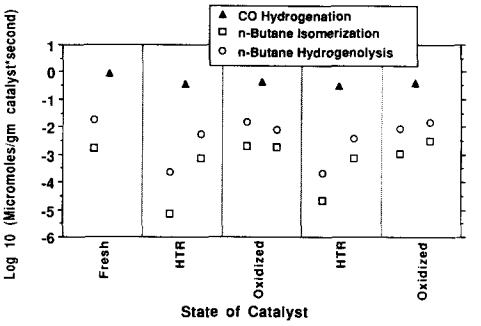

FIG. 8. Reaction rate as a function of catalyst pretreatment for PtT12a at T_{ref} = 553 K and P = 84.8 kPa (○, *n*-butane hydrogenolysis before and after CO hydrogenation; □, *n*-butane isomerization before and after CO hydrogenation; ▲, CO hydrogenation).

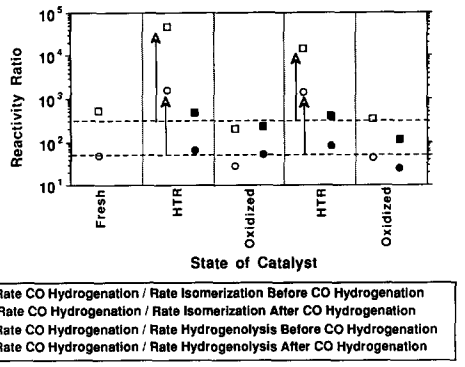

FIG. 9. Plot of the reactivity for PtT12a at T_{ref} = 553 K and P = 84.8 kPa using n-butane hydrogenolysis and isomerization reactivities before and after CO hydrogenation (○, CO hydrogenation/n-butane hydrogenolysis before CO hydrogenation; □, CO hydrogenation/n-butane isomerization before CO hydrogenation; ●, CO hydrogenation/n-butane hydrogenolysis after CO hydrogenation; ■, CO hydrogenation/n-butane isomerization after CO hydrogenation). Note the pronounced increase in both ratios for the HTR state and the recovery after CO hydrogenation.

sensitive reaction and, on supported Pt, the TOF increases with increasing dispersion (*19*). This behavior is corroborated in the results on $Pt/SiO_2$and Pt/Al_2O_3 reported in Figs. 2–5 and in Table 2. The hydrogenolysis activity per gram does not appear to be affected by high temperature reduction on either of these supports, indicating the absence of an SMSI state. Oxidation does, however, lead to a modest increase in activity which may be due to a "surface roughening" caused by preoxidation as seen previously on Rh catalysts (*18*). In contrast, n-butane isomerization and CO hydrogenation activities per gram of catalyst are unaffected by this oxidation treatment. The similarity in the behavior of n-butane isomerization and CO hydrogenation reactions is seen in the plot of their reactivity ratio (Fig. 6), which is unaffected by changes in particle diameter or by oxidation–reduction cycling.

The reactivity trends seen on the silica- and alumina-supported Pt can be used to interpret the results on the titania-supported catalyst. High temperature reduction in H_2 leads to a 2 orders of magnitude drop in hydrogenolysis activity. This drop in activity is significantly greater than the drop in activity on silica- and alumina-supported Pt after a comparable treatment and must be related to site blocking caused by the migration of TiO_x species from the support leading to the SMSI state, as proposed in the literature (*11–13*). A similar drop in activity is also seen in the isomerization of n-butane, but the activity for CO hydrogenation is unaffected by the high temperature reduction leading to the SMSI state. Since the ratio of CO hydrogenation to isomerization activity was unaffected by particle diameter or by oxidation–reduction treatments on silica and alumina supports, it is remarkable that the ratio is affected so dramatically by the HTR treatment on the titania support.

However, closer examination of Fig. 9 shows that it is only the ratio of CO hydrogenation activity to isomerization activity after HTR that is affected. When the isomerization activity of the catalyst after performing CO hydrogenation is considered, there is no effect of HTR on the reactivity ratio. Hence, this suggests that the TiO_x adspecies responsible for suppressed isomerization (and hydrogenolysis) activity have been removed from the surface during the CO hydrogenation reaction. Morris *et al.* (*26*) had previously suggested that since one of the products of the CO hydrogenation reaction, namely, H_2O, is known to reverse the SMSI state, it is likely that the catalyst during CO hydrogenation may not be in the SMSI state. Resasco and Haller (*27*) have provided quantitative evidence that when CO hydrogenation was performed in the SMSI state, no oxygenated products were seen initially. The oxygen coming from the CO molecule was presumably consumed by the support and led to oxidation of the TiO_x adspecies to TiO_2. Since oxidation of the surface leads to a reversal of the SMSI state, it is reasonable to assume that the very act of performing CO hydrogenation leads to a reversal of the SMSI state. Both hydrogenolysis and isomerization activity of n-butane,

which are suppressed strongly by the onset of the SMSI state, were restored after performing CO hydrogenation (Figs. 7 and 8), confirming the reversal of the SMSI state.

It is also interesting that high temperature reduction of Pt/TiO_2 did not lead to any change in the isomerization selectivity of *n*-butane despite a 2 orders of magnitude drop in activity per gram of catalyst. Isomerization selectivity is markedly affected by temperature, but we have eliminated this effect by performing all our measurements at a fixed temperature of 553 K or by extrapolating to this temperature. The results on silica- and alumina-supported Pt and those reported in Ref. (*19*) show that isomerization selectivity is a strong function of particle size. The relative insensitivity of isomerization selectivity to high temperature reduction leading to the SMSI state suggests that the changes taking place involve a decrease in the number of active sites without altering the nature of surface sites available. A similar conclusion was reached by Anderson *et al.* (*28*), who observed no change in isomerization selectivity for *n*-hexane conversion in the SMSI state. If the ensemble requirements for these reactions were markedly different, one would expect to see a change in isomerization selectivity as the surface is progressively covered with the TiO_x adspecies. These results argue strongly that the ensemble requirements for both these reactions are similar and that the activity suppression in the SMSI state is mainly due to site blocking.

Our results show that the support exerts a strong influence on the CO hydrogenation reaction rates. In contrast, the TOF for hydrogenolysis or isomerization of *n*-butane was, within the limits of experimental error, unaffected by the support (Table 2). As discussed above, the ratio of CO hydrogenation/*n*-butane isomerization activity truly reflects the intrinsic efficiency of Pt for these reactions since it was unaffected by particle size or pretreatment on both the silica and the alumina supports (Fig. 6). This reactivity ratio was also unaffected by the onset of the SMSI state, provided the isomerization reactivity of the catalyst after CO hydrogenation was considered. Hence, the SMSI state cannot be responsible for the enhancement in the CO hydrogenation rate on titania-supported Pt. The activity changes must therefore be a result of promotion by the support independent of the SMSI state since, in fact, the SMSI state was reversed during CO hydrogenation.

The increased reactivity for CO hydrogenation on titania-supported Pt was observed without any corresponding drop in hydrogenolysis or isomerization activity. Since hydrogenolysis and isomerization activity was strongly suppressed by the presence of Ti–suboxides on titania (as in the SMSI state), it is unlikely that the metal surface after CO hydrogenation is covered by a significant concentration of TiO_x species. We cannot rule out the possibility that mobile TiO_x species may migrate onto the metal surface during the CO hydrogenation reaction and lead to enhanced activity, but these species must subsequently wander off the surface since the TOFs for hydrogenolysis or isomerization of *n*-butane on Pt/TiO_2 are comparable to those on other supports. An alternative explanation for the enhanced CO hydrogenation activity may be the spillover of reactive intermediates onto the support and their subsequent reaction. This phenomenon has been termed surface site transfer by Glugla *et al.* (*29*) and causes a second methane desorption peak in TPR from CO + H_2 on Ni/Al_2O_3. On Pt/TiO_2, Mao and Falconer (*30*) see a similar spillover of reactive intermediates from Pt to the TiO_2 support resulting in an activity of Pt/TiO_2 approaching that of supported Ni. Robbins and Marucchi-Soos (*31*) have observed a similar phenomenon on Pt/Al_2O_3. They identified the reactive intermediate by FTIR to be a methoxy species. The evidence suggests that the methoxy intermediate can react on the TiO_2 or Al_2O_3 support to form methane and hence constitute an alternative pathway to methanation that may become kinetically

significant in the case of a poor methanation catalyst such as Pt.

The reactivity of Pt in the CO hydrogenation reaction increases in the order $Pt/SiO_2 < Pt/Al_2O_3 < Pt/TiO_2$. A similar increase in activity was also seen when the surface of Pt black was promoted by TiO_2 (*13*). The increased activity on Pt/TiO_2 is not related to the SMSI state as explained above but must be related to the availability of TiO_2 in the vicinity of the Pt metal particles. A similar increase in activity was seen when TiO_2 was deposited on the surface of Pt model catalysts in a UHV environment (*32*). The only discrepancy between the results on model catalysts and those on supported catalysts is the negative correlation between increased CO hydrogenation activity and the reactivity for hydrogenolysis of hydrocarbons (*33*). A similar negative correlation is not seen on supported catalysts. This difference can be understood in terms of the different morphology of the model and supported metal catalysts. On model single crystal catalysts, addition of TiO_2 on the surface increases the reactivity for CO hydrogenation but at the same time blocks surface sites. This leads to a maximum in reactivity with surface coverage of TiO_2. Removal of the oxide overlayers during CO hydrogenation may not be possible since there is no place for the TiO_2 to migrate to. On a supported catalyst, there is a large amount of titania in the vicinity of the metal particle which can assist in the CO hydrogenation reaction without blocking sites for hydrogenolysis. Hence the increase in CO hydrogenation activity on Pt supported on Al_2O_3 and TiO_2 supports is accomplished without any corresponding drop in reactivity for hydrogenolysis or isomerization of *n*-butane.

This study has also shown that highly dispersed Pt is not stable toward oxidation–reduction cycling on either of these supports. The particle size on the silica-supported catalysts increased from 1.5 to 4.0 nm after four cycles involving high temperature oxidation (823 K) treatments and HTR (773 K). On the alumina support, there was a more dramatic increase in particle diameter with three cycles, causing the particle size to go from 1.0 to 15.6 nm. The Pt particles were more stable on the titania support, increasing from 1.3 to 6.8 nm on PtT12a after six cycles and from 1.4 to 2.2 nm on PtTO4 after one cycle.

CONCLUSIONS

The ratio of CO hydrogenation/*n*-butane isomerization reactivity has been shown to be a very sensitive probe of the influence of the support. We have shown that this ratio is unaffected by particle size variations or by surface structure changes caused by oxidation–reduction cycling on a given support. Since the isomerization TOF was unaffected by the support, any variation in the reactivity ratio caused by going from one support to another must reflect the role of the support in enhancing the CO hydrogenation reaction. The results show that the reactivity ratio CO hydrogenation/*n*-butane isomerization goes from ≈ 3.5 on Pt/SiO_2 to ≈ 20 on Pt/Al_2O_3 and ≈ 300 on Pt/TiO_2.

The reversal of the SMSI state caused by CO hydrogenation implies that any oxide species that migrate over the metal surface during HTR cannot be responsible for the enhanced CO hydrogenation activity of these catalysts. If the enhanced activity of the TiO_2-supported catalysts is due to special interfacial sites at the metal–support interface, these sites must be present even on the catalyst in the LTR state and in the oxidized state. However, the similarity of the TOFs for *n*-butane hydrogenolysis on all the supports used in this study would argue against the presence of any oxide promoters on the metal surface in the TiO_2- or the Al_2O_3-supported catalysts. The results support the hypothesis that enhanced reactivity in the CO hydrogenation reaction on titania and alumina may be caused by spillover of reactive intermediates onto the support (*29–31*).

ACKNOWLEDGMENTS

Financial support for this work from the donors of the Petroleum Research Fund of the American Chemical Society, Grant 21168-AC5, is gratefully acknowledged. Transmission electron microscopy was performed at the electron beam microanalysis facility within the Department of Geology, University of New Mexico. High resolution microscopy was performed at the NSF HREM facility at Arizona State University, supported by Grant DMR 86-11609.

REFERENCES

1. Tauster, S. J., Fung, S. C., and Garten, R. L., *J. Amer. Chem. Soc.* **100**(1), 170 (1978).
2. Foger, K., *J. Catal.* **78,** 406 (1982).
3. Resasco, D. E., and Haller, G. L., *J. Catal.* **82,** 279 (1983).
4. Ko, E. I., and Garten, R. L., *J. Catal.* **68,** 233 (1981).
5. Braunschweig, E. J., Logan, A. D., Datye, A. K., and Smith, D. J., *J. Catal.* **118,** 227 (1989).
6. Bartholomew, C. H., Pannell, R. B., and Butler, J. L., *J. Catal.* **65,** 335 (1980).
7. Vannice, M. A., and Twu, C. C., *J. Catal.* **82,** 213 (1983).
8. Burch, R., and Flambard, A. R., *J. Catal.* **78,** 389 (1982).
9. Wang, S. Y., Moon, S. H., and Vannice, M. A., *J. Catal.* **71,** 167 (1981).
10. Taniguchi, S., Mori, T., Mori, Y., Hattori, T., and Murakami, Y., *J. Catal.* **119,** 108 (1989).
11. Santos, J., Phillips, J., and Dumesic, J. A., *J. Catal.* **81,** 147 (1983).
12. Sadeghi, H. R., and Henrich, V. E., *J. Catal.* **81,** 279 (1984).
13. Dwyer, D. J., Robbins, J. L., Cameron, S. D., Dudash, N., and Hardenbergh, J., *in* "Strong Metal Support Interactions," (R. T. K. Baker, S. J. Tauster, and J. A. Dumesic, Eds.), ACS Symp. Ser. Vol. 298, p. 21. Amer. Chem. Soc., Washington, DC, 1986.
14. Levin, M. E., Salmeron, M., Bell, A. T., and Somorjai, G. A., *J. Catal.* **106,** 401 (1987).
15. Anderson, J. B. F., and Burch, R., *Appl. Catal.* **25,** 173 (1986).
16. Logan, A. D., Braunschweig, E. J., Datye, A. K., and Smith, D. J., *Langmuir* **4,** 27 (1988).
17. Gao, S., and Schmidt, L. D., *J. Catal.* **111,** 210 (1988).
18. Braunschweig, E. J., Logan, A. D., Chakraborti, S., and Datye, A. K., *in* "Proceedings, 9th International Congress on Catalysis, Calgary, 1988" (M. J. Philips and M. Ternan, Eds.), p. 1122. Chem. Institute of Canada, Ottawa, 1988.
19. Rodríguez-Reinosos, F., Rodríguez-Ramos, I., Moreno-Castilla, C., Guerrero-Ruiz, A., and López-González, J. D., *J. Catal.* **107,** 1 (1987).
20. Davis, S. M., Zaera, F., and Samorjai, G. A., *J. Amer. Chem. Soc.* **104,** 7453 (1982).
21. Blankenburg, K. J., M.S. thesis, University of New Mexico, 1991.
22. Datye, A. K., Logan, A. D., Blankenburg, K. J., and Smith, D. J., *Ultramicroscopy,* **34,** 47 (1990).
23. Benesi, H. A., Curtis, R. M., and Studer, H. P., *J. Catal.* **10,** 328 (1968).
24. Messner, A. E., Rosie, D. M., and Argabright, P. A., *Anal. Chem.* **31**(2), 230, (February 1959).
25. Boudart, M., and McDonald, M. A., *J. Phys. Chem.* **88,** 2185 (1984).
26. Morris, S. R., Moyes, R. B., and Wells, P. B. *Stud. Surf. Sci. Catal.* **11,** 247 (1982).
27. Resasco, D. E., and Haller, G. L., *Adv. Catal.* **36,** 173 (1989).
28. Anderson, J. B. F., Burch, R., and Cairns, J. A., *J. Chem. Soc. Chem. Commun.*, 1648 (1986).
29. Glugla, P. G., Bailey, K. M., and Falconer, J. L., *J. Phys. Chem.* **92,** 4274 (1988).
30. Mao, T. F., and Falconer, J. L., *J. Catal.*, **123,** 443 (1990).
31. Robbins, J. L., and Marucchi-Soos, E., *J. Phys. Chem.* **93,** 2885 (1989).
32. Demmin, R. A., and Gorte, R. J., *J. Catal.* **105,** 373 (1987).
33. Williams, K. J., Levin, M. E., Salmeron, M., Bell, A. T., and Somorjai, G. A., *Catal. Lett.* **1,** 331 (1988).